Endocrinology, 2021, Vol. 162, No. 10, 1–14
https://doi.org/10.1210/endocr/bqab144
Research Article

Research Article

Pre-existing Thyroiditis Ameliorates Papillary Thyroid Cancer: Insights From a New Mouse Model

Fabiana Pani,[1] Yoshinori Yasuda,[1,2] Giulia Di Dalmazi,[3] Paulina Chalan,[1] Kathleen Gabrielson,[4] Luigi Adamo,[5] Elena Sabini,[1] Stefano Mariotti,[6] and Patrizio Caturegli[1]

[1]Division of Immunology, Department of Pathology, The Johns Hopkins School of Medicine, Baltimore, MD, USA; [2]Department of Endocrinology and Diabetes, Nagoya University Graduate School of Medicine, Nagoya, Japan; [3]Division of Endocrinology, Department of Medicine and Aging Sciences, "G. D'Annunzio" University of Chieti-Pescara, Chieti, Italy; [4]Department of Molecular and Comparative Pathobiology, Pathology and Oncology and Environmental Health Engineering Johns Hopkins School of Medicine and Bloomberg School of Public Health, Baltimore, MD, USA; [5]Division of Cardiology, Department of Medicine, The Johns Hopkins School of Medicine, Baltimore, MD, USA; and [6]Retired from Department of Medical Sciences and Public Health, University of Cagliari, Cagliari, Italy

ORCiD number: 0000-0003-2566-7971 (F. Pani); 0000-0002-0968-9954 (P. Chalan); 000-0001-6768-6308 (P. Caturegli).

Received: 5 March 2021; Editorial Decision: 5 July 2021; First Published Online: 31 July 2021; Corrected and Typeset: 26 August 2021.

Abstract

Papillary thyroid cancer (PTC) often co-occurs with Hashimoto's thyroiditis, an association that has long been reported in clinical studies yet remains controversial. Some studies, in fact, have suggested a protective effect of thyroiditis while others have not. We generated a mouse model where PTC and thyroiditis develop in a predictable manner, combining the oncogenic drive of the $BRAF^{v600E}$ mutation (inducible by tamoxifen) to the thyroiditis susceptibility of the $NOD.H2^{h4}$ strain (inducible by iodine). A total of 113 $NOD.H2^{h4}$_TPO-CRE-ER_$BRAF^{V600E}$ mice (50 followed throughout lifetime and 63 sacrificed at 16 weeks post tamoxifen) were used to determine whether the PTC phenotype differs when thyroiditis precedes or coincides with the onset of PTC. Mice with pre-existing thyroiditis lived longer (median survival of 28.2 weeks post tamoxifen) than those with concomitant (25.6 weeks) or no (24.5 weeks) thyroiditis ($P < 0.01$ by Laplace regression). PTC developed less frequently (33%) in the pre-existing thyroiditis group than the concomitant (100%) or no (100%) thyroiditis groups ($P < 0.001$ by chi-squared) and showed less aggressive histopathological features. The intratumoral mononuclear cell infiltration was more prominent in mice with pre-existing thyroiditis ($P = 0.002$ *vs* the other groups) and sustained by a significant expansion of effector memory CD8 + T cells and CD19 + B cells. These findings shed light on the controversial PTC-thyroiditis association and emphasize the contribution of intratumoral T and B lymphocytes to the evolution of PTC.

ISSN Online 1945-7170

Key Words: papillary thyroid cancer, carcinogenesis, autoimmune thyroiditis, thyroid antibodies

Papillary thyroid cancer (PTC), the most common thyroid neoplasia, arises from mutations that increase signaling through the mitogen-activated protein kinase pathway (1), notably the valine to glutamic acid change at codon 600 of the BRAF kinase (1). This mutation constitutively activates BRAF and drives cell transformation and proliferation in several type of cancers (2,3), such as hairy cell leukemia [100% prevalence, (4)], PTC [85% prevalence, (2)], melanoma [50% prevalence, (5)], colorectal cancer [10% prevalence, (6)], and nonsmall cell lung cancer [3% prevalence (7)]. PTC has low aggressiveness, with a 5-year survival of 100% when localizes to the thyroid gland or extends only to the regional lymph nodes and about 80% when metastasizes. PTC, however, represents a significant public health problem because its incidence, both in terms of asymptomatic and advanced-stage cases, is rising (8).

PTC has been known since 1955 (9) to associate with lymphocytic infiltration of the thyroid gland, an infiltration that often meets the pathological and clinical criteria of Hashimoto's thyroiditis, the most common human autoimmune disease (10). The PTC-thyroiditis association remains controversial but intellectually appealing especially in the light of the ever-increasing interest of oncologists in the immune system and the use of cancer immunotherapy. Some human studies have reported that thyroiditis reduces PTC incidence (11), clinical severity (12), and pathological aggressiveness (13), while others have reported the opposite findings (14,15). The reasons underlying these discrepancies are likely numerous, including different genetic backgrounds and demographics of the featured patients and difficulties in replicating the study cohorts and designs. Considering that the temporal relationship is one of the key criteria to assess causality and that the precise time of onset of thyroiditis and PTC is difficult to determine, we reasoned that a deeper understanding of the PTC-thyroiditis association could be gained by developing a mouse model where the 2 diseases are induced in a temporally defined fashion.

We performed a prospective cohort study in NOD.H2^{h4} mice to test the hypothesis that thyroiditis preceding the onset of PTC imparts different outcomes on PTC than thyroiditis developing concomitantly or subsequently to PTC.

Material and Methods

Mouse Strains and Experimental Groups

This new mouse model of PTC and thyroiditis was established by combining 3 strains: NOD.H2^{h4} congenic, TPO-CRE-ER transgenic, and BRAF^{V600E} knock-in mice. Breeding pairs of NOD.H2^{h4} congenic mice (H2^{g7}: K^{k}, A^{k}, E^{0}, D^{b}) were a gift of Dr. George Carayanniotis (Memorial University of Newfoundland, St. Johns, Canada). Similar to the parental NOD strain, the best animal model for type 1 diabetes, the NOD.H2^{h4} is considered the model that most faithfully mimics Hashimoto thyroiditis: these mice develop thyroiditis spontaneously, with an incidence that increases and is accelerates by the addition of sodium iodide to the drinking water (16,17). In this study, we indicated the model of spontaneous autoimmune thyroiditis accelerated by iodine as iodine exacerbated thyroiditis (IET). Breeding pairs of TPO-CRE-ER transgenic mice, which express the viral CRE recombinase fused to a portion of the human estrogen receptor under control of the thyroperoxidase promoter, were a gift of Dr. David McFadden (Internal Medicine and Biochemistry, UT Southwestern, Dallas, TX, USA) (18). BRAF knock-in mice, which carry the V600E mutation in exon 15 (19), were purchased from the Jackson Laboratory (stock no. 017837). The genomic structure of the TPO-CRE-ER and loxP BRAF alleles is shown in Supplemental Figure 1A and 1B, respectively (20). The 2 strains, originally made on the C57BL6 background (H2-b: K^{b}, A^{b}, E^{b}, D^{b}), were backcrossed onto the NOD.H2^{h4} background for 20 and 16 generations, respectively, to confer susceptibility to thyroiditis [Supplemental Figure 2A (20)].

After this extensive backcrossing, TPO-CRE-ER transgenic and BRAF^{V600E} knock-in mice were intercrossed for 2 generations to obtain the desired genotype [Supplemental Figure 2B (20)]: heterozygous TPO-CRE-ER and homozygous BRAF^{V600E}, indicated in this study as NOD.H2^{h4}_TPO-CRE-ER_BRAF^{V600E}. A total of 113 NOD.H2^{h4}_TPO-CRE-ER_BRAF^{V600E} mice (60 males and 53 females) were generated and used in this study: they develop IET when drinking iodine-supplemented water and PTC when injected with tamoxifen.

The 113 NOD.H2^{h4}_TPO-CRE-ER_BRAF^{V600E} mice were divided into 3 experimental groups (Fig. 1A). In 1 group [concomitant IET, n = 33 (22 tamoxifen and 11 corn oil)], iodine administration and tamoxifen (or corn oil) injections were begun at the same time when mice were 8 weeks old. In a second group [pre-existing IET, n = 34 (22 tamoxifen and 12 corn oil)], thyroiditis was induced first, starting iodine at week 8 and continued for 12 weeks, and then tamoxifen (or corn oil) injections were started when mice were 20 weeks old. In a third group [no IET, n = 46, 22 tamoxifen and 24 corn oil)], no iodine was given and tamoxifen (or corn oil) injections began at 8 weeks of age.

The 113 NOD.H2^{h4}_TPO-CRE-ER_BRAF^{V600E} mice were analyzed in 2 different follow-up modalities (hereafter: cohorts). The first cohort of 50 NOD.H2^{h4}_TPO-CRE-ER_BRAF^{V600E} mice (lifetime cohort) was used to define the natural history of PTC. It comprised 31 mice injected with tamoxifen and 19 with corn oil. Mice in this cohort were followed up to the time of their natural death or up to when euthanasia was requested by the animal facility veterinarians (due to ruffled fur, reduced motility, and/or a body weight loss > 20%). Serial thyroid ultrasound analyses of this lifetime cohort demonstrated that PTC consistently developed by 16 weeks after the first tamoxifen injection. Therefore, the second cohort of 63 mice (16-week cohort) was sacrificed at 16 weeks post tamoxifen to collect the experimental end points. It comprised 35 mice injected with tamoxifen and 28 with corn oil. The sex and cohort distribution of all 113 mice is summarized in Supplemental Table 1 (20).

To establish baseline comparisons for thyroid hormones and thyroid antibodies in the NOD.H2^{h4}_TPO-CRE-ER_BRAF^{V600E} mice, we also used 22 nongenetically modified NOD.H2^{h4} mice (10 with synchronous iodine supplementation and tamoxifen injections and 12 mice only injected with tamoxifen).

All studies were performed under a protocol approved by the Institutional Animal Care and Use Committee of the Johns Hopkins University.

Screening of the Mouse Colony

PCR genotyping on tail DNA for both TPO-CRE-ER transgene and BRAFV600E mutations

DNA was extracted from by digesting a small tail clip with a 10 mg/mL solution of proteinase K (Thermo Fisher Scientific EO0491) for 30 minutes at 37°C. DNA was then amplified by PCR using conditions and primers indicated in Supplemental Table 2 (20). Representative PCR screening results are shown in Supplemental Figure 3A and 3B (20).

Thyroidal expression of CRE mRNA

To verify the expression of CRE recombinase in thyroid follicular cells, total thyroid RNA was extracted by TRIZOL reagent (Sigma-Aldrich 93289) according to manufacturer's instructions and then reverse transcribed using oligo (dT)18 (Thermo Fisher Scientific SO131). The resulting complementary DNA was then amplified using FAST SYBR^{TM} Green PCR Master Mix (Thermo Fisher Scientific 4385612) using CRE-specific primers [listed in Supplemental Table 2 (20)]. A representative real-time PCR experiment is shown in Supplemental Figure 3C and 3D (20).

Selection of the NOD.H2h4 background by MHC class II typing of peripheral blood mononuclear cells

During backcrossing, to enrich for the NOD.H2^{h4} background (which features the k allele at the MHC class II

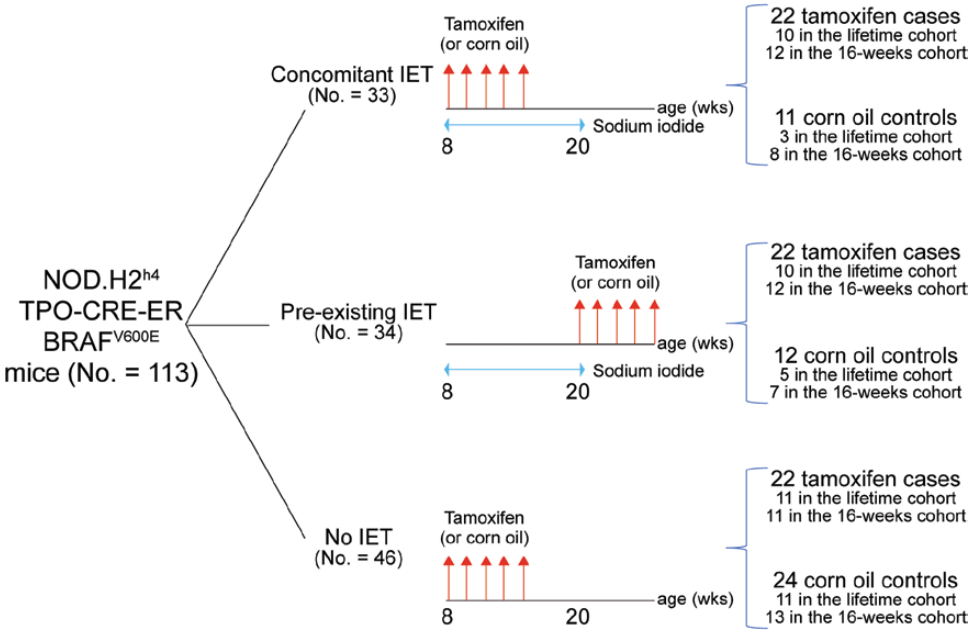

Figure 1. Study design. A total of 113 NOD.H2^{h4}_TPO-CRE-ER_BRAF^{V600E} mice were assigned to 3 experimental groups: 1 where thyroiditis and papillary thyroid cancer (PTC) were induced concomitantly (by sodium iodide supplementation to the drinking water and tamoxifen injection, respectively); 1 where thyroiditis was induced first and then followed by PTC induction; and 1 where only PTC was induced. Each group contained 1 arm where mice were injected with tamoxifen and another where they were injected with vehicle control (corn oil). Injections are indicated by red arrows. The 113 mice were analyzed in 2 follow-up modalities: the first 50 mice (lifetime cohort, 31 injected with tamoxifen and 19 corn oil) were followed-up until their natural death (or up to when euthanasia was requested by veterinarians); the second 63 mice (16-week cohort, 35 injected with tamoxifen and 28 corn oil) were sacrificed at 16 weeks after the first tamoxifen injection.

A locus) (16), peripheral blood mononuclear cells were purified, treated with BD FACS erythrocyte lysing solution, and stained for 30 min at 4°C using antibodies directed against CD45, MHC class I K^b, and MHC class II A^k [Supplemental Table 3 (20)]. Cells were analyzed using a BD LSR II flow-cytometer and FlowJo software (version 10.1). Representative flow cytometry panels are shown in Supplemental Figures 3E to 3H (20).

Induction of PTC and Autoimmune Thyroiditis

PTC was induced administering tamoxifen via injection in animals between 8 and 20 weeks of age. Tamoxifen (Sigma-Aldrich T5648-1G) was added to corn oil at a concentration of 25 mg/mL and dissolved by overnight incubation at 37°C. Each mouse was injected intraperitoneally with 100 µL of this solution once a day for 5 consecutive days. Since 8-week-old NOD.H2^{h4} have an average body weight of 20 g, this dose corresponds to approximately 125 mg tamoxifen per kg of body weight.

The spontaneous autoimmune thyroiditis typical of the NOD.H2^{h4} strain was exacerbated by supplementing the drinking water with 2 g/L of sodium iodide (Sigma-Aldrich, 217638-100G). This supplementation began when mice were 8 weeks old and continued for 12 consecutive weeks.

Serum Thyroid Antibodies, Total Thyroxine, and Thyroid-stimulating Hormone

To define the reference range for thyroglobulin antibodies, thyroperoxidase antibodies, total thyroxine (T4) and thyroid stimulating hormone (TSH), we analyzed 135 8-week-old NOD.H2^{h4} mice. Thyroglobulin antibodies were measured by enzyme-linked immunosorbent assay using a previously developed in-house assay (21). We identified 44 AU/mL as the 95th percentile, and therefore values exceeding this threshold were defined as elevated. Thyroperoxidase antibodies were measured by flow cytometry using a Chinese Hamster Ovary cell line stably transfected with the mouse thyroperoxidase complementary DNA, a cell line kindly donated by Dr. Sandra McLachlan (22). We identified 12% as the 95th percentile for thyroglobulin antibodies, and therefore values exceeding this threshold were defined as elevated [Supplemental Figure 4 A-D (20)].

Serum levels of total T4 and TSH were measured using a Luminex bead assay as previously reported (21). TSH ranged from 71 to 747 pg/mL (5th to 95th percentile), and T4 ranged between 109 and 260 ng/mL (5th to 95th percentile).

Serum thyroid antibodies, serum total thyroxine, and TSH were assessed in 78 NOD.H2^{h4}_TPO-CRE-ER_BRAF^{V600E} mice.

Thyroid Ultrasound

To characterize noninvasively the presence and extent of thyroid cancer in mice, we used a Vevo 2100 microimaging ultrasound system (Visual Sonics, Toronto, ON, Canada). Since the mouse thyroid is located approximately 1 cm under the skin, we used the transducer with the highest frequency (MS700 embryonic probe; 30-70 MHz) to achieve the required penetration. Prior to ultrasound scanning, mice were anesthetized (inhalation of 2.5% isoflurane) and depilated in the neck region (Nair depilatory cream). The thyroid was then analyzed using a transaxial planes to obtain anteroposterior (depth) and laterolateral (width) dimensions, also implementing color Doppler analysis. We scored thyroid echogenicity and nodules to quantify the risk of thyroiditis and/or thyroid cancer, using the same criteria used in humans to classify autoimmune thyroiditis (23) and thyroid cancer [Thyroid Imaging, Reporting and Data System (TI-RADS) (24,25) criteria]. These criteria are summarized in Supplemental Table 4 (20).

Thyroid Histopathology and Immunohistochemistry

At sacrifice, thyroid glands were resected and prepared for histopathology [hematoxylin and eosin (H&E) and immunohistochemistry] and/or flow cytometry. For H&E histopathology, the thyroid glands or lobes were fixed overnight in Beckstead's zinc solution (26) and then embedded in paraffin. Thyroid blocks were cut at 5 µm, obtaining sections that were stained by H&E. Using a digital microscope (Olympus BX43) equipped with the Cell Sens Standard software, images were scored for PTC and thyroiditis. PTC was quantified in term of size and number, obtaining an area representing the percent involvement of the total thyroid area (27), as well as intratumoral mononuclear cell infiltration, graded from 0 (none) to 3 (extensive). Thyroiditis was scored from 0 to 4 according to the involvement of the thyroid lobes by infiltrating hematopoietic mononuclear cells, as previously described (28). For immunohistochemistry, thyroid sections were deparaffinized and rehydrated as described (29), and then staining using the following primary antibodies: F4/80 for macrophages, PAX8 and TTF-1 for thyroid-specific genes, Ki67 for cell proliferation, and cleaved caspase 3 for apoptosis [antibody details are provided in Supplemental Table 3 (20)].

Flow Cytometry

The entire thyroid gland or 1 lobe was digested to prepare a single cell suspension, as previously described (21). Briefly, the tissue was minced and digested for 2 h at 4°C and then for 30 min at 37°C in a solution of RPMI 1640. The single cell suspension was treated with Fc Block and stained with the following antibodies at 1:200 concentration: CD45 (Biolegend 103132), CD3 (Biolegend 100236), CD4 (Biolegend 116016), CD8 (Biolegend 100723), CD44 (Biolegend 103047), CD62L (Biolegend 104407), CD19 (Biolegend 115529), immunoglobin D (Biolegend 405729), and immunoglobin M (Biolegend 406517) [Supplemental Table 3 (20)]. Samples were analyzed on a BD LSR II flow cytometer, and data were analyzed using FlowJo software (version 10.1; Tree Star). The gating strategy used is reported in Supplemental Figure 5 (20).

Statistical Analysis

Experimental groups were compared using the Kruskal-Wallis test followed by 2-way comparisons adjusted for multiple comparisons. Binary categorical variables were compared by chi-squared test. Ordinal categorical variables were compared by Wilcoxon's rank sum test and continuous variables by *t* test or rank sum test as appropriate. Kaplan-Meier nonparametric survival analysis followed by log-rank test and Laplace regression were used to compare mortality across experimental groups. The longitudinal serum levels of thyroid hormones and thyroid antibodies were assessed using multiple linear regression with generalized estimating equations to take into account the fact that measures repeated over time in the same mice are likely to be correlated with one another. In addition to the experimental group (the main predictor), the model also included sex and days of follow-up.

P-values < 0.05 indicated statistical significance. Analyses were performed using Stata statistical software, release 16.1 (Stata, College Station, TX, USA).

Results

Pre-existing Iodine-induced Thyroiditis Decreases PTC Incidence and Severity and Prolongs Survival

In the lifetime cohort (50 mice: 31 injected with tamoxifen and 19 with corn oil), overall survival was significantly longer in mice with pre-existing IET than in those with concomitant or no IET ($P < 0.001$ by log rank test) (Fig. 2A). The median survival was 28.2 weeks (95% CI 26.7-29.7 weeks) in the pre-existing IET group, as compared to 25.6 and 24.5 weeks in the other 2 groups ($P < 0.01$ by Laplace regression). All 31 tamoxifen-injected mice of the lifetime cohort ultimately developed PTC (100% incidence), as compared to 5 of 19 (26%) corn oil–injected mice (2 in the pre-existing IET and 3 in the no IET group ($P < 0.001$ by chi-squared test) (Fig. 2B). PTC, as assessed by H&E histopathology, differed in size and morphology among the groups. In particular, the median (mean) percentage thyroid area involved by PTC was 54% (56%), 53% (50%), and 26% (38%) in the tamoxifen injected mice (concomitant, pre-existing, and no IET, respectively), while 0% (0%), 0% (8%), and 0% (7%) in the corn oil–injected mice (Fig. 2C). Therefore, PTC was more prevalent and larger in mice injected with tamoxifen than in those injected with corn oil and did not significantly differ by thyroiditis onset in term of incidence and size when assessed at the end of the mouse lifetime.

The 16-weeks cohort (63 mice: 35 mice injected with tamoxifen and 28 with corn oil) confirmed and refined the results obtained from the lifetime cohort. As before, the incidence of PCT was, predictably, greater in mice injected with tamoxifen than in those injected with corn oil ($P < 0.001$ by chi-squared). But in this cohort, PTC was less frequent and smaller in mice of the pre-existing IET group. In particular, the incidence of PTC was 33% (4 of 12) as compared to 100% in the concomitant (12 of 12) or no (11 of 11) IET groups ($P < 0.001$ by chi-squared) (Fig. 2B). The thyroid area involved by PTC was also significantly smaller in the pre-existing IET group, with a median (mean) of 0% (7%), as compared to 50% (51%) in the concomitant IET group and 33% (37%) in the no IET group ($P < 0.001$ by Wilcoxon rank sum test) (Fig. 2D). Overall, these results indicate that pre-existing IET delayed the onset of PTC mediated by $BRAF^{V600E}$ mutation and decreased its aggressiveness.

PTC Exhibits More Favorable Ultrasonographic, Macroscopic, and Histopathological Features in Mice With Pre-existing Iodine-induced Thyroiditis

Thyroid ultrasound performed serially in mice of the 16-weeks cohort showed marked differences in PTC appearance among the experimental groups. Mice of the concomitant IET group injected with tamoxifen showed nodules markedly suspicious for malignancy (Fig. 3A), which had in most of the cases (8 of 12) a TI-RADS score of 5 (Table 1). Nodules were surrounded by a moderately hypoechogenic thyroid parenchyma, which had a thyroiditis score of 2 in most mice (11 of 12) (Table 1). Gross examination showed nodules emerging from an enlarged thyroid gland, which was difficult to dissect because firmly attached to surrounding tissues (Fig. 3B). Histopathological examination revealed the classical features of PTC, as well as spindle

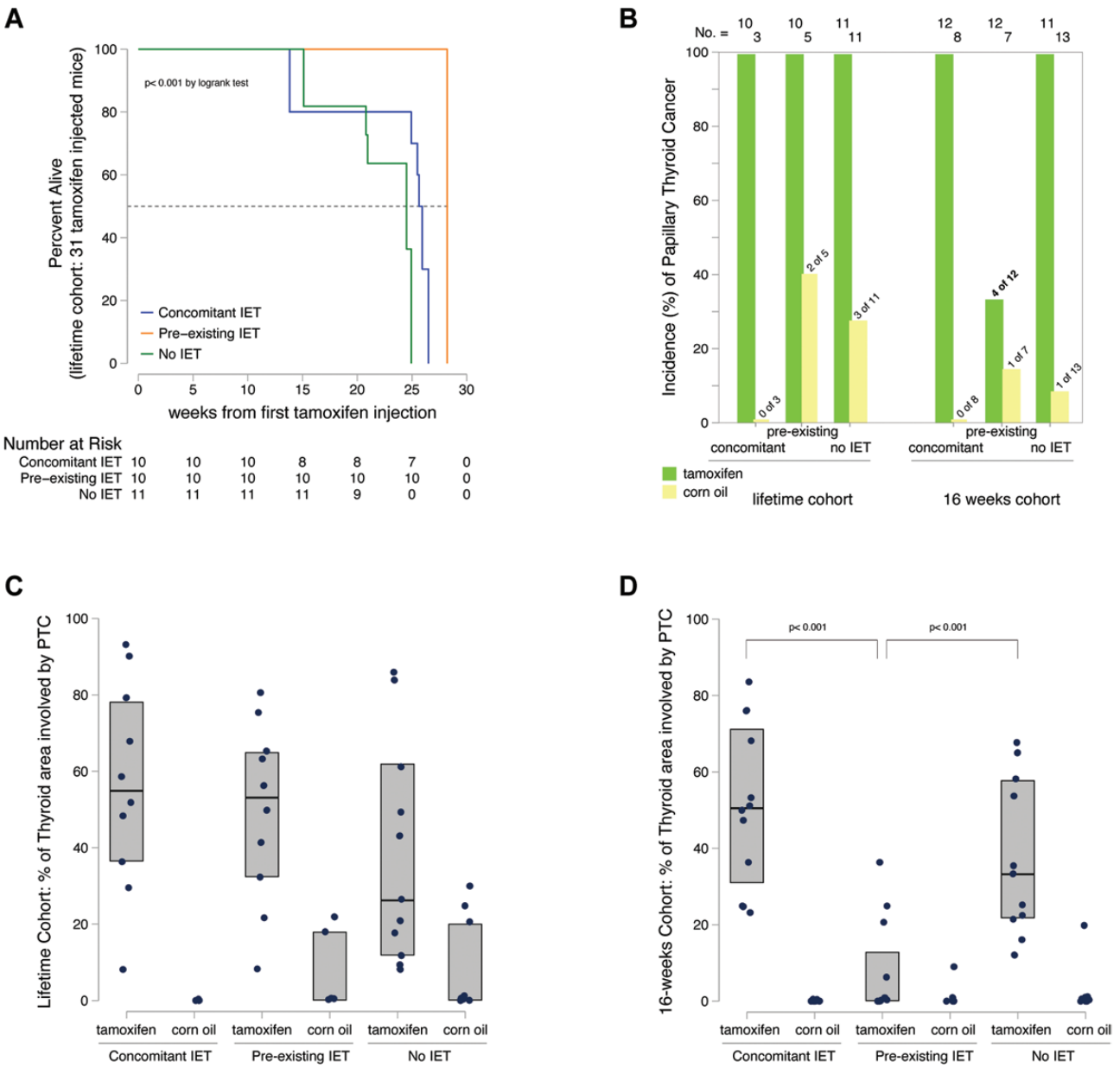

Figure 2. The phenotype of papillary thyroid cancer is ameliorated by pre-existing thyroiditis. (A) Survival curve of the 31 mice in the lifetime cohort injected with tamoxifen, according to the experimental group. Overall survival is compared by the log rank test; median survival (dashed line) by Laplace regression. (B) Incidence of papillary thyroid cancer in all 113 NOD.H2^{h4}_TPO-CRE-ER_BRAF^{V600E} mice featured in the study, according to cohort type (lifetime or 16 weeks), experimental group [concomitant, pre-existing, or no iodine-exacerbated thyroiditis (IET)], and injection type (tamoxifen or corn oil). Differences in the distribution of incidence were compared by chi-squared test. (C) Severity of papillary thyroid cancer (PTC) in the 50 mice of the lifetime cohort. (D) Severity of PTC in the 63 mice of the 16-week cohort. Severity was expressed as percent of the total thyroid area involved by PTC. Comparisons among groups were done Kruskal Wallis test, followed by the Wilcoxon rank sum test for pairwise assessments.

cells, which are found in the poorly differentiated variant (Fig. 3C). At the rim of the thyroid parenchyma, a very small area of lymphocytic infiltration was also found (Fig. 3D). PTC lesions were multicentric in most of the mice (9 of 12; 75%) (Table 2). Animals in the same cohort but in the corn oil control arm showed features indicative of thyroiditis (score of 2) without PTC (Fig. 3 E-3H; Table 1).

Mice of the pre-existing IET group injected with tamoxifen exhibited severe hypoechogenicity as the main ultrasonographic finding, with thyroiditis score of 3 present in 9 of the 12 mice (Table 1). This feature was accompanied by an enlarged thyroid gland containing numerous nodules with benign morphology that were difficult to identify in the context of the hypoechogenic background (Fig. 3I). These nodules in most cases had low TI-RADS scores (Table 1) and upon gross examination displayed irregular texture without a clearly distinct nodular structure (Fig. 3J). Histopathology

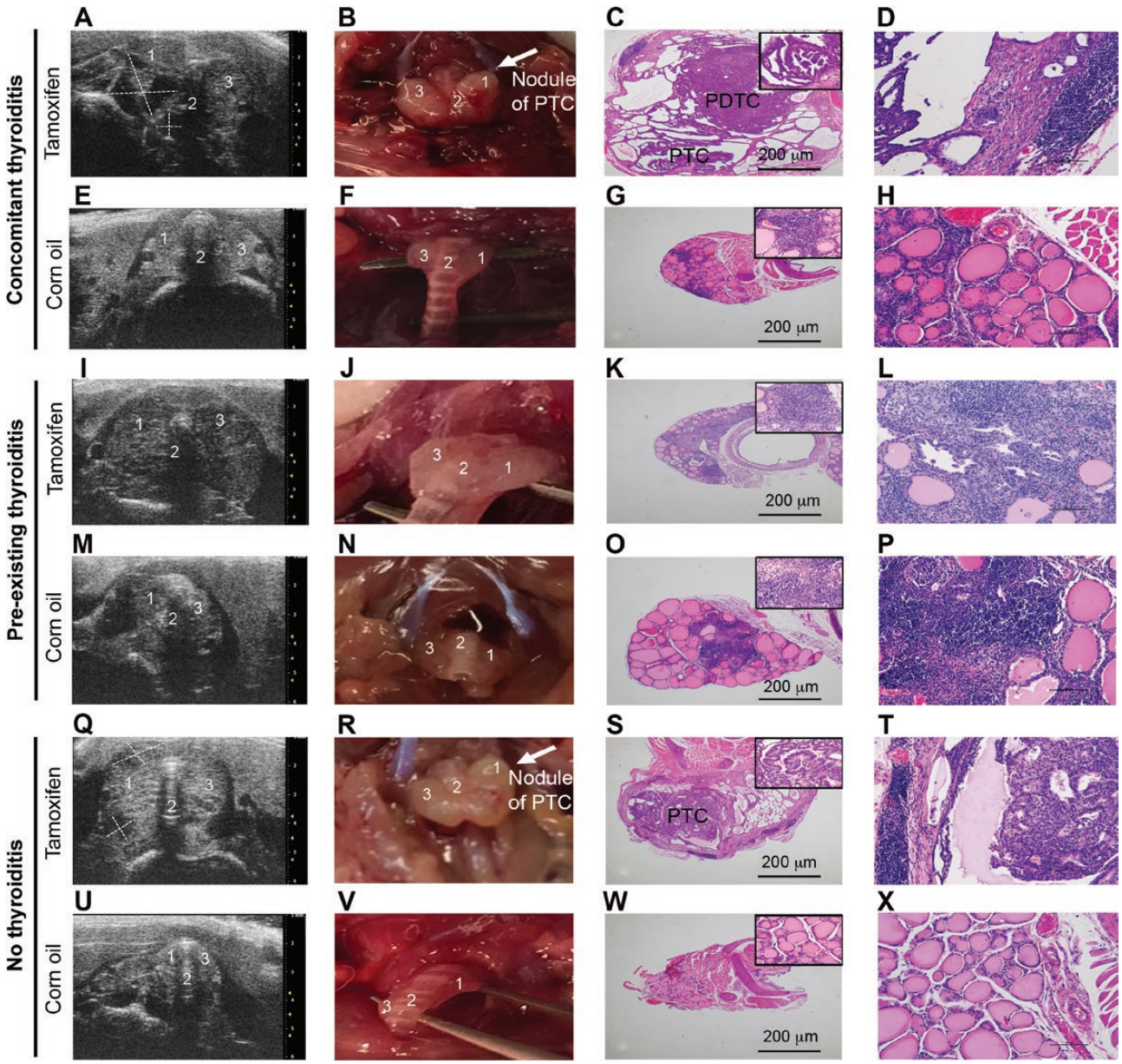

Figure 3. Ultrasonographic, macroscopic, and histopathological features of the thyroid gland in the three experimental groups. The left column (A, E, I, M, Q, U) shows thyroid ultrasonographic images; the second column (B, F, J, N, R, V) shows the gross morphology of the mouse thyroid glands and surrounding cervical areas at the time of dissection; the third column (C, G, K, O, S, W) shows hematoxylin and eosin histopathology; and the fourth column represents a high-power magnification of the area marked on the images in the third column. Each pair of rows represents mice injected with tamoxifen (top row) or vehicle (bottom row) in the 3 experimental groups: concomitant thyroiditis, pre-existing thyroiditis, and no thyroiditis. PTC indicates a papillary thyroid carcinoma while PDTC indicates a poorly differentiated cancer with features of papillary thyroid carcinoma. 1 = right thyroid lobe, 2 = isthmus of the thyroid, 3 = left thyroid lobe.

revealed microfoci of PTC surrounded by a severe diffuse area of lymphocytic infiltration (Fig. 3K-3L). Strikingly, none of these mice developed multicentric PTC lesions, having instead 1 (5 of 12) or no (7 of 12) nodules ($P = 0.001$) (Table 2). Corn oil controls for this group showed a marked area of mononuclear lymphocytic thyroiditis (Fig. 3M-3P).

Mice of the no IET group injected with tamoxifen showed ultrasonographic nodules suspicious for malignancy that were similarly surrounded by a moderately hypoechogenic parenchyma, although the highest TI-RADS malignancy score was less prevalent (7 of 11; 63%) (Table 1; Fig. 3Q). These nodules appeared malignant by gross examination (Fig. 3R), without capsular invasion (Fig. 3S). PTC lesions were multicentric but with lower prevalence than in the concomitant thyroiditis group (7 of 12; 58%) (Table 2). The rim of thyroid parenchyma was also surrounded by a very small area of lymphocytic infiltration (Fig. 3T). Corn

Table 1. Thyroiditis score and TI-RADS in the 63 NOD TPO-CRE-ER-BRAF^{v600E} mice of the 16-week cohort, according to the experimental group (concomitant, pre-existing, or no iodine-exacerbated thyroiditis)

		Thyroiditis score				TI-RADS				
	Mice (n)	0	1	2	3	1	2	3	4	5
Concomitant IET										
Tamoxifen	12	0	0	11	1	2	0	0	2	8
Corn oil	8	0	0	8	0	8	0	0	0	0
Pre-existing IET										
Tamoxifen	12	0	0	3	9	4	1	3	3	1
Corn oil	7	0	0	3	4	6	0	1	0	0
No IET										
Tamoxifen	11	0	2	9	0	1	0	1	2	7
Corn oil	13	0	7	6	0	10	0	3	0	0

Abbreviations: IET, iodine exacerbated thyroiditis; TI-RADS, Thyroid Imaging, Reporting, and Data System.

Table 2. Focality of papillary thyroid cancer in the 63 NOD TPO-CRE-ER-BRAF^{v600E} mice of the 16-week cohort, according to the experimental group (concomitant, pre-existing, or no iodine-exacerbated thyroiditis)

		Papillary thyroid cancer foci		
	Mice (n)	0	1	≥2
Concomitant IET				
Tamoxifen	12	0	3	9
Corn oil	8	8	0	0
Pre-existing IET				
Tamoxifen	12	7	5	0
Corn oil	7	6	1	0
No IET				
Tamoxifen	11	1	3	7
Corn oil	13	12	1	0

Abbreviation: IET, iodine exacerbated thyroiditis.

oil control mice of this experimental showed a preserved thyroid gland structure without lymphocytic infiltration, with mild to moderate hypoechogenicity and nodules with TI-RADS not greater than 3 (Table 1; Fig. 3U-3X).

Thyroid Glands of Mice With Pre-existing Iodine-induced Thyroiditis Feature a Unique Expansion of CD19^{+} B Cells and CD8^{+} Effector Memory T Cells

To further characterize the mononuclear cell subsets infiltrating, we analyzed by flow cytometry and immunohistochemistry thyroid glands resected from a subset of 18 tamoxifen injected mice of the 16-week cohort (6 in each of the 3 groups). Thyroids from the pre-existing IET group showed an increased percentage and absolute number (cells per mg of thyroid) of CD3 + T cells and CD19 + B cells. The median [interquartile range (IQR)] CD3 + T cells was in fact 34% (4%), as compared to 11% (3%) in the concomitant and 5% (2%) in the no IET groups ($P = 0.004$ *vs* concomitant ; $P = 0.002$ *vs* no IET by Wilcoxon rank sum test) (Fig. 4A). For CD19 + B cells, the median (IQR) was 30% (11%) in the pre-existing IET group, while 8% (3%) in the concomitant and 3% (1%) in the no IET group ($P = 0.002$ *vs* concomitant; $P = 0.002$ *vs* no IET by Wilcoxon rank sum test) (Fig. 4B). The intrathyroidal lymphoid subset that differed among groups the most was the effector memory CD8 T cells, defined by the expression of CD44 and absence of CD62L. This subset, known to mediate protective host immune responses (30), increased in both percentage and absolute number in the thyroids of mice from the pre-existing IET group. The median (IQR) percentage was 41% (7%) as compared to 17% (15%) in the concomitant and 16% (20%) in the no IET groups ($P = 0.002$ *vs* concomitant and *vs* no IET by Wilcoxon rank sum test) (Fig. 4C). A representative thyroid CD44 *vs* CD62L CD8 + T cell profile from a mouse of the 3 experimental groups is shown in Figure 4D to 4F.

The F4/80 staining for macrophages showed clear but sparse infiltrating cells in the thyroid affected by PTC, with no difference among experimental groups [Supplemental Figure 6 (20)], overall suggesting a marginal role of macrophages in the immune response against PTC in this mouse model.

Thyroid Antibodies, Especially Those Against Thyroperoxidase, Are Associated With the Onset of PTC

Thyroglobulin antibodies developed, as expected (17), upon iodine administration at about 3 to 4 weeks from the start (11-12 weeks of age), reached the zenith at 12 weeks post iodine initiation, and then declined over the ensuing months (Fig. 5A and 5B). They also developed in mice not receiving iodine supplementation in drinking water, due to the thyroiditis-prone NOD.H2^{h4} background, albeit at lower titers (Fig. 5C). Thyroglobulin antibody seroconversion was largely independent of tamoxifen or corn oil injection (compare closed to open symbols) but paralleled the development of PTC. They, in fact, peaked at the time of PTC appearance (16 weeks after the first injection) and remained more elevated in tamoxifen injected mice than in corn oil controls, both in the pre-existing (Fig. 5A) or concomitant (Fig. 5B) IET groups.

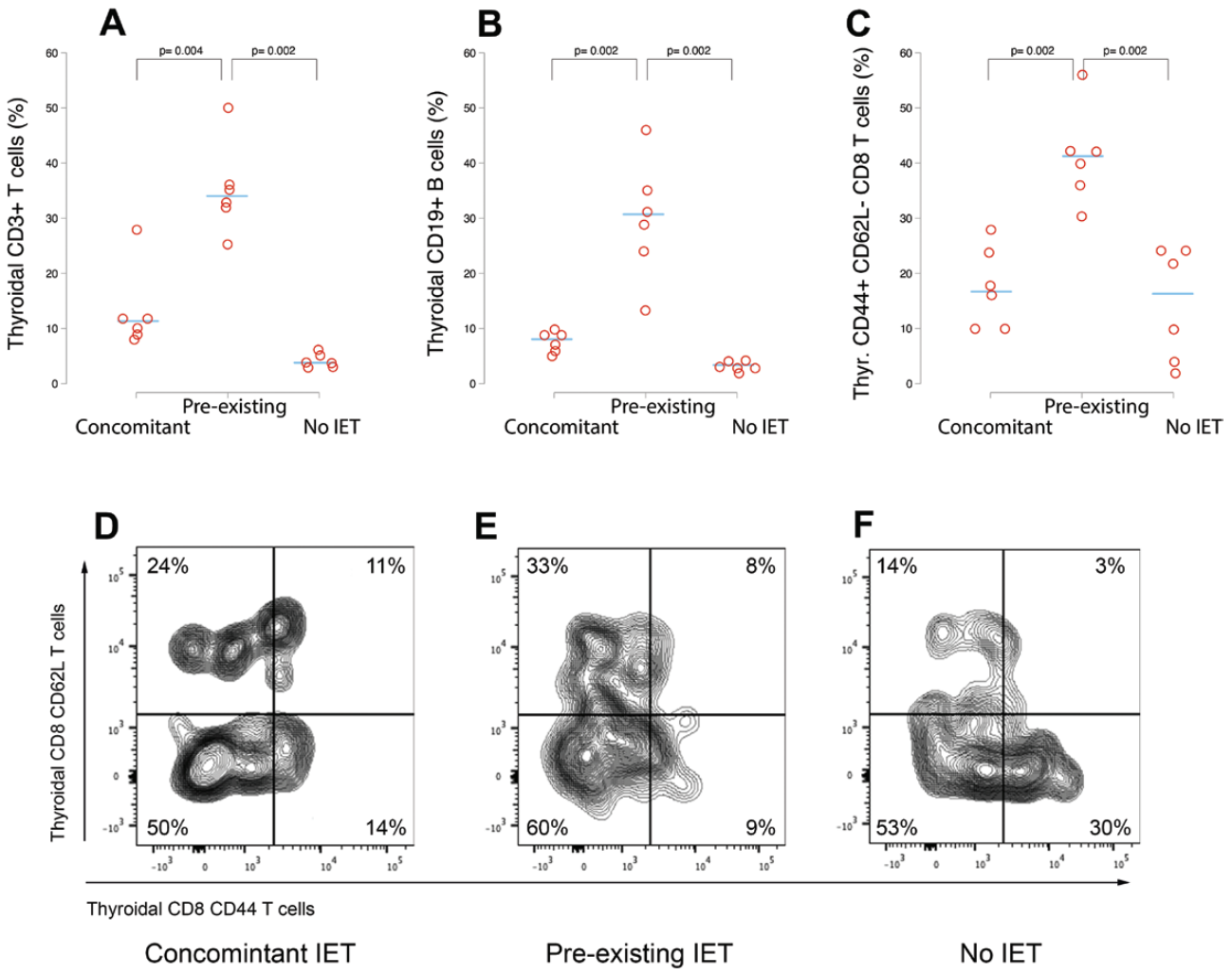

Figure 4. Expansion of T cells, B cells, and CD44 + CD62L- CD8 +T cells in the thyroid of mice with pre-existing thyroiditis. (A) Thyroid CD3 +T cells (percentage of the total, live CD45 positive cells) in the 3 experimental groups. (B) Thyroid CD19 + B cells (percentage of the total, live CD45 positive cells). (C) Thyroid CD44 + CD62L- CD8 +T cells (percentage of the total CD3 + CD8 +T cells). The horizontal bars indicate the median percentage. (D-F) Representative flow cytometry plots of the thyroid CD8 T cells, according to the expression of CD62L and CD44. The single CD62L population represents naïve T cells; the double positive population the central memory T cells; the single CD44 positive population the effector memory T cells; and the double negative population the exhausted T cells.

Thyroperoxidase antibodies began to appear later than thyroglobulin antibodies (around 20 weeks of age) independently of iodine supplementation and showed higher titers in tamoxifen treated mice developing PTC. In animals with pre-existing IET (Fig. 5D) and no IET (Fig. 5F) this increase reached statistical significance. A similar trend was observed in mice with concomitant IET, but the difference did not reach statistical significance ($P = 0.7$).

Primary Hypothyroidism Develops Upon Induction of PTC but Is Greatly Attenuated in Mice With Pre-existing Iodine-induced Thyroiditis

When PTC was detected (16 weeks after tamoxifen injection), serum TSH significantly increased in all tamoxifen-injected groups (Table 3), but this increase was markedly more pronounced in mice with concomitant and no IET when compared to corn oil controls ($P = 0.0012$ and $P = 0.0002$, respectively). On the contrary, serum TSH only slightly increased in mice with pre-existing IET with no significant difference when compared to corn oil controls ($P = 0.5$).

Overall, these data suggest that hypothyroidism in this animal model is the consequence of thyroid invasion and destruction by PTC rather than the result of thyroid autoimmunity.

Serum T4 tended to decrease in all mice injected with tamoxifen although it became significantly lower only in those with concomitant and no IET ($P = 0.0068$ and $P = 0.0001$ respectively).

Thyroid glands retained the expression of the thyroid-specific genes PAX-8 and TTF-1 and showed moderate

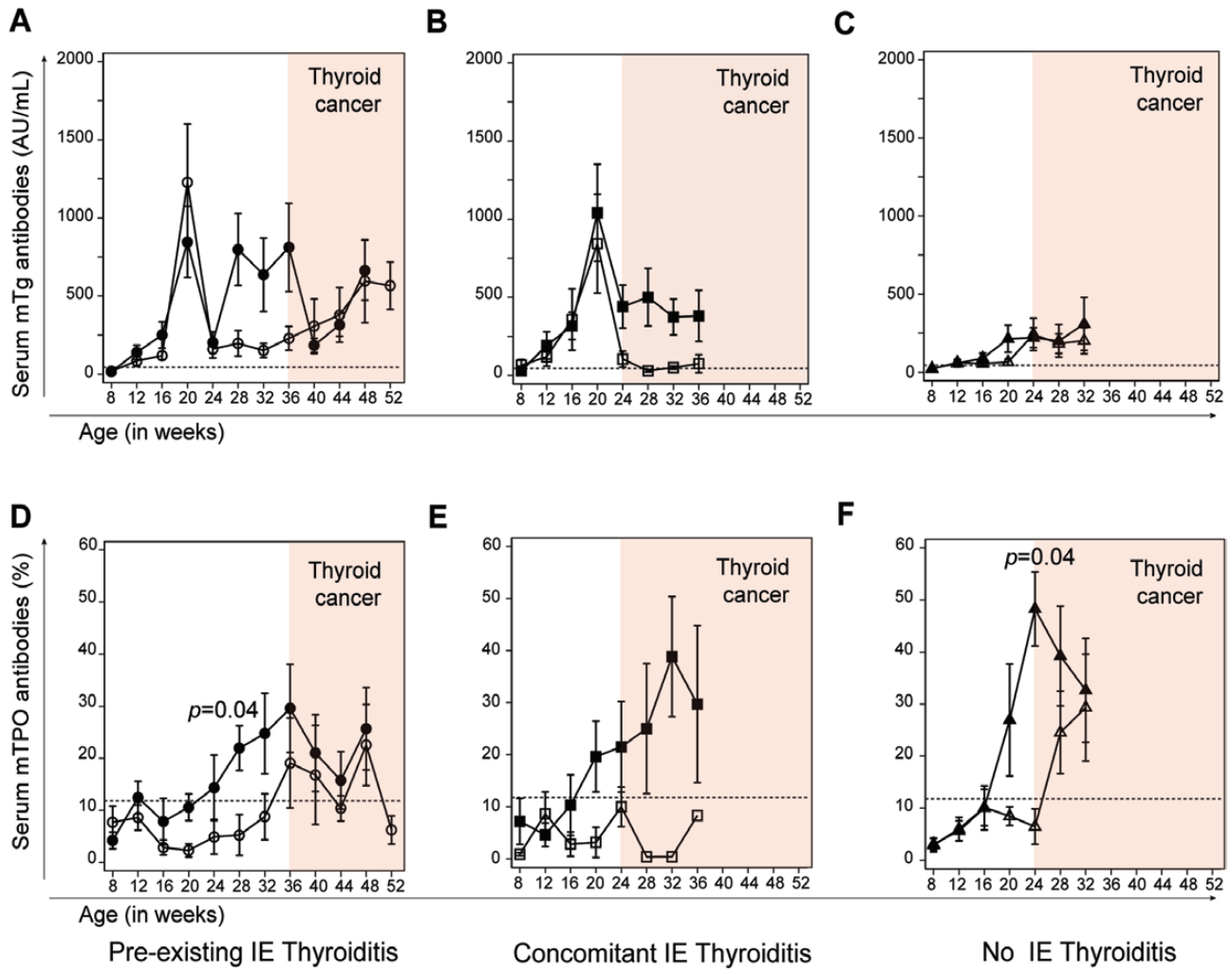

Figure 5. Serum thyroid antibodies. (A-C) Serum antibodies against mouse thyroglobulin (mTg). (D-F) Serum antibodies against mouse thyroperoxidase (mTPO) in the 3 experimental groups (concomitant, pre-existing, and no iodine-exacerbated thyroiditis). Filled symbols indicate mice injected with tamoxifen, while open symbols mice injected with vehicle control (corn oil). Dashed lines indicate the upper limit of the normal reference range. The red shaded areas mark the time after development of papillary thyroid cancer.

evidence of cell proliferation or apoptosis (as assessed by Ki67 and cleaved caspase 3 expression, respectively), with no differences among the groups [Supplemental Figure 7 (20)].

Discussion

We report the development and characterization of a mouse model that assesses the interaction between thyroiditis and PTC. We found that pre-existing and concomitant thyroiditis have markedly different effects on the natural history of PTC: pre-existing thyroiditis is protective while concomitant thyroiditis is not. These findings shed light on the long-standing controversial relationship between thyroiditis and PTC. Some studies found a protective role, but many others an aggressive behavior. Radetti et al (11) confirmed a protective effect of thyroiditis in a cohort of 904 children with Hashimoto's thyroiditis who were followed for up to 13 years. In this study, although a significant percentage of subjects (174; 19%) developed thyroid nodules, only 10 of 904 (about 1%) were malignant (8 papillary and 2 follicular). However, other studies found the opposite. Using the Taiwanese Health Insurance database, Chen et al (15) identified 1521 newly diagnosed thyroiditis cases between 1998 and 2010 and 6084 frequency-matched controls. They reported that patients with thyroiditis had a 12-fold increased risk of PTC than nonthyroiditis controls. Boi et al (14) confirmed these findings in a cytological series of 484 patients followed for up to 6 years, reporting that PTC associated with thyroiditis had greater multifocality, capsular and vascular invasion, and enhanced papillary features.

When thyroiditis preceded the onset of $BRAF^{V600E}$-mediated PTC, it prolonged survival of mice follow

Table 3. Thyroid function in NOD TPO-CRE-ER-BRAF^{V600E} mice according to the experimental group

		Serum TSH (pg/mL)			Serum total T4 (ng/mL)		
	Mice (n)	Baseline	PTC diagnosis	*P*-value vs baseline	baseline	PTC diagnosis	*P*-value *vs* baseline
Concomitant IET							
Tamoxifen	14	265 ± 248	15830 ± 12979	<0.001	161 ± 39	68 ± 49	<0.001
Corn oil	6	295 ± 202	893 ± 1472	0.347	164 ± 46	143 ± 52	0.476
Pre-existing IET							
Tamoxifen	14	214 ± 113	679 ± 956	0.082	183 ± 47	182 ± 83	0.969
Corn oil	8	256 ± 93	645 ± 732	0.158	160 ± 103	157 ± 90	0.951
No IET							
Tamoxifen	17	370 ± 332	9454 ± 11015	0.002	176 ± 44	107 ± 49	<0.001
Corn oil	17	411 ± 349	264 ± 267	0.002	180 ± 41	242 ± 113	0.041

Blood was collected at baseline and at the time ultrasonographic evidence of papillary thyroid cancer was first established
Abbreviations: IET, iodine exacerbated thyroiditis; PTC, papillary thyroid cancer; TSH, thyroid-stimulating hormone.

throughout their lifetime. This beneficial effect was associated with a larger mononuclear cell infiltrate in the thyroid gland, suggesting that the thyroid inflammation might have a tumor controlling effect. This protective effect of pre-existing IET was confirmed and expanded when mice were euthanized at a predefined time point after PTC initiation. In fact, mice with pre-existing thyroiditis showed a delay in the development of PTC (Fig. 2B) and developed fewer PTC nodules and of smaller size and focality (Table 2; Fig. 3) than animals that developed thyroiditis synchronously with PTC. We found that animals with pre-existing IET had a high thyroiditis score and low TI-RADS score (Table 1). This recapitulates findings in humans that highlighted a reverse correlation between ultrasound-based thyroiditis score and TI-RADS score (31). Overall, these findings provide a framework to interpret the apparently conflicting reports on the relationship between Hashimoto's thyroiditis and PTC, protective (12,32) *vs* not protective (14,33). Our work also confirms the utility of thyroid ultrasound for the characterization of PTC nodules (18,34-36).

Pre-existing thyroiditis was associated with a higher peritumoral and intratumoral mononuclear cell infiltration (Table 3). It is interesting to speculate on the mechanisms underlying the protective effect of pre-existing thyroiditis and ascribe it to the extent and composition of the lymphoid infiltrate in the thyroid gland. Cellular immune responses, mainly those mediated by CD8 T cells, are in fact classically considered key mediators of antitumor immune surveillance (15,22,32,37). These effector tumor-infiltrating lymphocytes have been extensively characterized in several solid tumors (38,39), including those of the thyroid gland (40-43) and are often classified into functional subsets that are, however, not distinctly homogenous and separable. Recent thymic emigrants that have not encountered their antigen yet (naïve T cells) lack the expression of CD44 and CD62L and travel from blood to the various lymphoid stations. Upon antigen encounter, they differentiate into effector cells; that is, they acquire the ability to produce cytokines and other mediators, carry out their function, and then die after a few days. Some of these effector cells become central memory T cells: they share the same trafficking pattern of naïve T cells (from blood to lymph nodes and then back to blood) but acquire the expression of both CD44 and CD62L as well as CCR7, which make them particularly suited for homing to T-cell–rich areas of secondary lymphoid organs. Some of the antigen-primed, central memory T cells lose the expression of CD62L and CCR7 and specialize in rapidly entering inflamed peripheral tissues, such as organs targeted by autoimmunity or harboring cancer. This subset, called effector memory T cells, is the prime mediator of effector functions and strongly expand upon antigen restimulation and secrete large amounts of inflammatory cytokines. We found that a distinctive feature of thyroid tumor-infiltrating lymphocytes from mice with pre-existing thyroiditis was the expansion of effector memory CD8 T cells (Fig. 5) and thus propose it as an important event that halts or delays the onset and progression of PTC. Recently, studies focused on understanding the mechanistic basis of immune checkpoint inhibitors antitumor effects have highlighted an important role of B cells in the context of tumor immune surveillance (44). The increase in thyroidal B cells associated with pre-existing thyroiditis that we observed (Fig. 4) could therefore also be an important event that contributes to immune mediated control of PTC. In other words, we suggest that pre-existing thyroid autoimmunity equips the host with the necessary tools to eliminate cancerous cells once they arise or to limit their expansion.

Serum antibodies directed against thyroglobulin in patients with PTC are considered either a reflection of coexisting autoimmune thyroiditis or the response of the immune system to newly emerged tumor associated

epitopes (45). In the mouse model presented in this study, we observed an initial peak of thyroglobulin antibodies that reflected the response to dominant and/or cryptic iodinated epitopes (17), a response that gradually faded with ceasing of the iodine supplementation (Fig. 5). The long-term persistence of thyroglobulin antibodies in tamoxifen-treated mice, however, suggests a true association of these antibodies with PTC development, possibly resulting from the appearance of novel, tumor-related epitopes within the large thyroglobulin molecule. Thyroperoxidase antibodies, the more specific serological marker of autoimmune thyroiditis in both patients (46) and NOD.H2^{h4} mice (22), also were found to associate with PTC development in our study. These antibodies, in fact, consistently appeared at higher titers in tamoxifen-treated mice that developed PTC, independently of the administration of iodine (Fig. 5).

In our study, all tamoxifen-injected mice developed TSH elevation, which was significant, however, only in animals where thyroiditis and PTC were induced synchronously or in those in which thyroiditis was not induced by iodine. Thus, in our animal model, primary hypothyroidism was not due to autoimmunity but was rather the consequence of normal thyroid disruption and invasion by nonfunctioning neoplastic cells. This result is in keeping both with the classical IET model induced in NOD.H2^{h4} strain, where the mice remain mostly euthyroid (47) and with several models of BRAF^{V600E} driven thyroid tumors, which are associated with severe primary hypothyroidism (48,49). On the other hand, the marked increase of TSH occurring in mice with concomitant or absent IET could contribute to the cancer progression observed in these experimental groups, considering the important role of this hormone in thyroid cancer growth (18,36,49-51).

Our study has some limitations. First, thyroid carcinogenesis in this model, where multiple thyroid cells are predicted to express the BRAF^{V600E} mutation upon action of the CRE recombinase, is likely different from the one of humans, where lesions most often represent clonal expansion of a single mutated cells. Moreover, although a powerful tool for researchers, CRE/estrogen receptor system might also have the potential to induce cancer without tamoxifen injection (leakiness), and this effect must be controlled for experimental design (52). Another limitation is that the thyroiditis induced in this model, although based on an autoimmune susceptible background such as the NOD.H2^{h4} mouse, relies on extremely high doses of iodine, which are rarely encountered in the clinical arena. Thus, the murine iodine-induced thyroiditis is likely immunologically different from the thyroiditis Hashimoto's patients develop so this experimental plan should be considered cautiously. Furthermore, this animal model has been established as a reliable experimental method to induce IET in an acceptable timeframe (17). In addition, in the pre-existing IET group, PTC was induced 12 weeks later than in the 2 other cohorts to keep consistent the timing of induction of thyroiditis. This might have unpredictable effects on tumor growth and progression. Finally, our flow cytometric characterization of the immune milieu of the PTC in the various cohorts studied is based on the analysis of a small number of animals. The results reported, at least in terms of percentages, are in line with observations made in samples of thyroid tissue collected from many more mice while optimizing the flow cytometric panel. However, the post-hoc pairwise comparisons in many cases only tended toward statistical significance and findings from the analysis of small groups of animals must always be interpreted with attention.

In conclusion, we report a novel mouse model of thyroiditis and PTC where the interaction between these 2 diseases can be explored. While thyroiditis that develops at the same time of PTC influences minimally its course, a pre-existing thyroiditis markedly decreases PTC incidence and severity, indicating a critical role of the immune system in PTC pathogenesis. Additional studies will be needed to further characterize this interaction and refine the use of cancer immunotherapy drugs based the presence and onset of thyroiditis in patients with PTC.

Acknowledgments

Author Contributions: P.C. directed the project and designed research; F.P., Y.Y., G.D.D., P.C., E.S., and K.G. performed research; F.P., P.C., S.M., and L.A. analyzed data; and F.P., L.A., S.M., and P.C. wrote the paper.

Financial Support: The experiments were supported in part by National Institutes of Health grant R01 CA194042 and in part by patient donations to the Johns Hopkins Autoimmune Disease Research Center. Fabiana was supported in part by a grant from the Italian Ministry of Education (grant number 2012Z3FHE); E.S. by the Virginia O'Leary & John C. Wilson Autoimmune Disease Research Fellowship; P.C. by the Walter and Jean Boek Autoimmune Research Fellowship.

Additional Information

Correspondence: Patrizio Caturegli, MD, MPH, Johns Hopkins Pathology, Ross Building, Room 656, 720 Rutland Avenue, Baltimore, MD 21205, USA. Email: pcat@jhmi.edu.

Disclosure Summary: The authors have declared that no direct conflict of interest exists.

Data Availability: Some or all data generated or analyzed during this study are included in this published article or in the data repositories listed in references.

References

1. Fagin JA, Wells SA Jr. Biologic and clinical perspectives on thyroid cancer. *N Engl J Med*. 2016;**375**(11):1054-1067.
2. Ciampi R, Nikiforov YE. Alterations of the BRAF gene in thyroid tumors. *Endocr Pathol*. 2005;**16**(3):163-172.
3. Davies H, Bignell GR, Cox C, et al. Mutations of the BRAF gene in human cancer. *Nature*. 2002;**417**(6892):949-954.
4. Falini B, Martelli MP, Tiacci E. BRAF V600E mutation in hairy cell leukemia: from bench to bedside. *Blood*. 2016;**128**(15):1918-1927.
5. Gray-Schopfer V, Wellbrock C, Marais R. Melanoma biology and new targeted therapy. *Nature*. 2007;**445**(7130):851-857.
6. Tejpar S, Bertagnolli M, Bosman F, et al. Prognostic and predictive biomarkers in resected colon cancer: current status and future perspectives for integrating genomics into biomarker discovery. *Oncologist*. 2010;**15**(4):390-404.
7. Leonetti A, Facchinetti F, Rossi G, et al. BRAF in non-small cell lung cancer (NSCLC): Pickaxing another brick in the wall. *Cancer Treat Rev*. 2018;**66**:82-94.
8. Lim H, Devesa SS, Sosa JA, Check D, Kitahara CM. Trends in thyroid cancer incidence and mortality in the United States, 1974-2013. *JAMA*. 2017;**317**(13):1338-1348.
9. Dailey ME, Lindsay S, Skahen R. Relation of thyroid neoplasms to Hashimoto disease of the thyroid gland. *AMA Arch Surg*. 1955;**70**(2):291-297.
10. McLeod DS, Caturegli P, Cooper DS, Matos PG, Hutfless S. Variation in rates of autoimmune thyroid disease by race/ethnicity in US military personnel. *JAMA*. 2014;**311**(15):1563-1565.
11. Radetti G, Loche S, D'Antonio V, et al. Influence of hashimoto thyroiditis on the development of thyroid nodules and cancer in children and adolescents. *J Endocr Soc*. 2019;**3**(3):607-616.
12. Castagna MG, Belardini V, Memmo S, et al. Nodules in autoimmune thyroiditis are associated with increased risk of thyroid cancer in surgical series but not in cytological series: evidence for selection bias. *J Clin Endocrinol Metab*. 2014;**99**(9):3193-3198.
13. Moon S, Chung HS, Yu JM, et al. Associations between hashimoto thyroiditis and clinical outcomes of papillary thyroid cancer: a meta-analysis of observational studies. *Endocrinol Metab (Seoul)*. 2018;**33**(4):473-484.
14. Boi F, Pani F, Calò PG, Lai ML, Mariotti S. High prevalence of papillary thyroid carcinoma in nodular Hashimoto's thyroiditis at the first diagnosis and during the follow-up. *J Endocrinol Invest*. 2018;**41**(4):395-402.
15. Chen YK, Lin CL, Cheng FT, Sung FC, Kao CH. Cancer risk in patients with Hashimoto's thyroiditis: a nationwide cohort study. *Br J Cancer*. 2013;**109**(9):2496-2501.
16. Podolin PL, Pressey A, DeLarato NH, Fischer PA, Peterson LB, Wicker LS. I-E+ nonobese diabetic mice develop insulitis and diabetes. *J Exp Med*. 1993;**178**(3):793-803.
17. Kolypetri P, King J, Larijani M, Carayanniotis G. Genes and environment as predisposing factors in autoimmunity: acceleration of spontaneous thyroiditis by dietary iodide in NOD.H2(h4) mice. *Int Rev Immunol*. 2015;**34**(6):542-556.
18. McFadden DG, Vernon A, Santiago PM, et al. p53 constrains progression to anaplastic thyroid carcinoma in a Braf-mutant mouse model of papillary thyroid cancer. *Proc Natl Acad Sci U S A*. 2014;**111**(16):E1600-E1609.
19. Dankort D, Filenova E, Collado M, Serrano M, Jones K, McMahon M. A new mouse model to explore the initiation, progression, and therapy of BRAFV600E-induced lung tumors. *Genes Dev*. 2007;**21**(4):379-384.
20. Pani F, Yasuda Y, Di Dalmazi G, et al. Supplemental data for: Pre-existing thyroiditis ameliorates papillary thyroid cancer: insights from a new mouse model. Deposited June 17, 2021. *Zenodo*. doi:10.5281/zenodo.4977012
21. Di Dalmazi G, Chalan P, Caturegli P. MYMD-1, a novel immunometabolic regulator, ameliorates autoimmune thyroiditis via suppression of Th1 responses and TNF-α release. *J Immunol*. 2019;**202**(5):1350-1362.
22. Chen CR, Hamidi S, Braley-Mullen H, et al. Antibodies to thyroid peroxidase arise spontaneously with age in NOD.H-2h4 mice and appear after thyroglobulin antibodies. *Endocrinology*. 2010;**151**(9):4583-4593.
23. Rago T, Cantisani V, Ianni F, et al. Thyroid ultrasonography reporting: consensus of Italian Thyroid Association (AIT), Italian Society of Endocrinology (SIE), Italian Society of Ultrasonography in Medicine and Biology (SIUMB) and Ultrasound Chapter of Italian Society of Medical Radiology (SIRM). *J Endocrinol Invest*. 2018;**41**(12):1435-1443.
24. Russ G, Bonnema SJ, Erdogan MF, Durante C, Ngu R, Leenhardt L. European thyroid association guidelines for ultrasound malignancy risk stratification of thyroid nodules in adults: the EU-TIRADS. *Eur Thyroid J*. 2017;**6**(5):225-237.
25. Grani G, Lamartina L, Ascoli V, et al. Reducing the number of unnecessary thyroid biopsies while improving diagnostic accuracy: toward the "right" TIRADS. *J Clin Endocrinol Metab*. 2019;**104**(1):95-102.
26. Beckstead JH. A simple technique for preservation of fixation-sensitive antigens in paraffin-embedded tissues: addendum. *J Histochem Cytochem*. 1995;**43**(3):345.
27. LiVolsi VA. Papillary thyroid carcinoma: an update. *Mod Pathol*. 2011;**24**(Suppl 2):S1-S9.
28. Caturegli P, Rose NR, Kimura M, Kimura H, Tzou SC. Studies on murine thyroiditis: new insights from organ flow cytometry. *Thyroid*. 2003;**13**(5):419-426.
29. Kuiper HM, Brouwer M, Linsley PS, van Lier RA. Activated T cells can induce high levels of CTLA-4 expression on B cells. *J Immunol*. 1995;**155**(4):1776-1783.
30. Martin MD, Badovinac VP. Defining memory CD8 T cell. *Front Immunol*. 2018;**9**:2692.
31. Zhou H, Yue WW, Du LY, et al. A modified thyroid imaging reporting and data system (mTI-RADS) for thyroid nodules in coexisting Hashimoto's thyroiditis. *Sci Rep*. 2016;**6**:26410.
32. Kebebew E, Treseler PA, Ituarte PH, Clark OH. Coexisting chronic lymphocytic thyroiditis and papillary thyroid cancer revisited. *World J Surg*. 2001;**25**(5):632-637.
33. Iliadou PK, Effraimidis G, Konstantinos M, et al. Chronic lymphocytic thyroiditis is associated with invasive characteristics of differentiated thyroid carcinoma in children and adolescents. *Eur J Endocrinol*. 2015;**173**(6):827-833.
34. Greco A, Albanese S, Auletta L, et al. High-frequency ultrasound-guided injection for the generation of a novel orthotopic mouse model of human thyroid carcinoma. *Thyroid*. 2016;**26**(4):552-558.

35. Nikitski AV, Rominski SL, Condello V, et al. Mouse model of thyroid cancer progression and dedifferentiation driven by STRN-ALK expression and loss of p53: evidence for the existence of two types of poorly differentiated carcinoma. *Thyroid*. 2019;**29**(10):1425-1437.
36. Gunda V, Gigliotti B, Ndishabandi D, et al. Combinations of BRAF inhibitor and anti-PD-1/PD-L1 antibody improve survival and tumour immunity in an immunocompetent model of orthotopic murine anaplastic thyroid cancer. *Br J Cancer*. 2018;**119**(10):1223-1232.
37. Caturegli P, De Remigis A, Rose NR. Hashimoto thyroiditis: clinical and diagnostic criteria. *Autoimmun Rev*. 2014;**13**(4-5):391-397.
38. Kawata A, Une Y, Hosokawa M, Uchino J, Kobayashi H. Tumor-infiltrating lymphocytes and prognosis of hepatocellular carcinoma. *Jpn J Clin Oncol*. 1992;**22**(4):256-263.
39. Kolbeck PC, Kaveggia FF, Johansson SL, Grune MT, Taylor RJ. The relationships among tumor-infiltrating lymphocytes, histopathologic findings, and long-term clinical follow-up in renal cell carcinoma. *Mod Pathol*. 1992;**5**(4):420-425.
40. Bagnasco M, Venuti D, Paolieri F, Torre G, Ferrini S, Canonica GW. Phenotypic and functional analysis at the clonal level of infiltrating T lymphocytes in papillary carcinoma of the thyroid: prevalence of cytolytic T cells with natural killer-like or lymphokine-activated killer activity. *J Clin Endocrinol Metab*. 1989;**69**(4):832-836.
41. Galdiero MR, Varricchi G, Marone G. The immune network in thyroid cancer. *Oncoimmunology*. 2016;**5**(6):e1168556.
42. Lee RS, Schlumberger M, Caillou B, Pages F, Fridman WH, Tartour E. Phenotypic and functional characterisation of tumour-infiltrating lymphocytes derived from thyroid tumours. *Eur J Cancer*. 1996;**32A**(7):1233-1239.
43. Ozaki O, Ito K, Mimura T, Sugino K, Hosoda Y. Papillary carcinoma of the thyroid. Tall-cell variant with extensive lymphocyte infiltration. *Am J Surg Pathol*. 1996;**20**(6):695-698.
44. Hollern DP, Xu N, Thennavan A, et al. B cells and T follicular helper cells mediate response to checkpoint inhibitors in high mutation burden mouse models of breast cancer. *Cell*. 2019;**179**(5):1191-1206.e21.
45. Latrofa F, Ricci D, Vitti P, et al. Characterization of thyroglobulin epitopes in Sardinian adults and juveniles with Hashimoto's thyroiditis: evidence against a major effect of age and genetic background on B-cell epitopes. *Clin Endocrinol (Oxf)*. 2010;**73**(1):110-113.
46. Mariotti S, Caturegli P, Piccolo P, Barbesino G, Pinchera A. Antithyroid peroxidase autoantibodies in thyroid diseases. *J Clin Endocrinol Metab*. 1990;**71**(3):661-669.
47. Teng X, Shan Z, Teng W, Fan C, Wang H, Guo R. Experimental study on the effects of chronic iodine excess on thyroid function, structure, and autoimmunity in autoimmune-prone NOD.H-2h4 mice. *Clin Exp Med*. 2009;**9**(1):51-59.
48. Knauf JA, Ma X, Smith EP, et al. Targeted expression of BRAFV600E in thyroid cells of transgenic mice results in papillary thyroid cancers that undergo dedifferentiation. *Cancer Res*. 2005;**65**(10):4238-4245.
49. Orim F, Bychkov A, Shimamura M, et al. Thyrotropin signaling confers more aggressive features with higher genomic instability on BRAF(V600E)-induced thyroid tumors in a mouse model. *Thyroid*. 2014;**24**(3):502-510.
50. Knauf JA, Luckett KA, Chen KY, et al. Hgf/Met activation mediates resistance to BRAF inhibition in murine anaplastic thyroid cancers. *J Clin Invest*. 2018;**128**(9):4086-4097.
51. Fiore E, Vitti P. Serum TSH and risk of papillary thyroid cancer in nodular thyroid disease. *J Clin Endocrinol Metab*. 2012;**97**(4):1134-1145.
52. Kristianto J, Johnson MG, Zastrow RK, Radcliff AB, Blank RD. Spontaneous recombinase activity of Cre-ERT2 in vivo. *Transgenic Res*. 2017;**26**(3):411-417.